Mon. Not. R. Astron. Soc. **000**, 1–10 (2014) Printed 29 January 2014 (MN LATEX style file v2.2)

Evolution of the extinction curves in galaxies

Ryosuke S. Asano[1⋆†], Tsutomu T. Takeuchi[1], Hiroyuki Hirashita[2] and Takaya Nozawa[3]
[1]*Department of Particle and Astrophysical Science, Nagoya University, Furo-cho, Chikusa-ku, Nagoya 464-8602, Japan*
[2]*Institute of Astronomy and Astrophysics, Academia Sinica, P. O. Box 23-141, Taipei 10617, Taiwan*
[3]*Kavli Institute for the Physics and Mathematics of the Universe (WPI), University of Tokyo, Kashiwa, Chiba 277-8583, Japan*

arXiv:1401.7121v1 [astro-ph.GA] 28 Jan 2014

Accepted **. Received **; in original form **

ABSTRACT

We investigate the evolution of extinction curves in galaxies based on our evolution model of grain size distribution. In this model, we considered various processes: dust formation by SNe II and AGB stars, dust destruction by SN shocks in the ISM, metal accretion onto the surface of grains (referred to as grain growth), shattering and coagulation. We find that the extinction curve is flat in the earliest stage of galaxy evolution. As the galaxy is enriched with dust, shattering becomes effective to produce a large abundance of small grains ($a \lesssim 0.01$ μm). Then, grain growth becomes effective at small grain radii, forming a bump at $a \sim 10^{-3}$–10^{-2} μm on the grain size distribution. Consequently, the extinction curve at ultraviolet (UV) wavelengths becomes steep, and a bump at $1/\lambda \sim 4.5$ $\mu\mathrm{m}^{-1}$ (λ : wavelength) on the extinction curve becomes prominent. Once coagulation becomes effective, the extinction curves become flatter, but the UV extinction remains overproduced when compared with the Milky Way extinction curve. This discrepancy can be resolved by introducing a stronger contribution of coagulation. Consequently, an interplay between shattering and coagulation could be important to reproduce the Milky Way extinction curve.

Key words: dust, extinction – galaxies: evolution – galaxies: ISM – ISM: clouds – galaxies: general – stars: formation

1 INTRODUCTION

Dust grains are one of the fundamental ingredients for understanding the formation and evolution of galaxies. The surface of dust grains is the main site for the formation of hydrogen molecules (e.g., Cazaux & Tielens 2004), which act as an effective coolant in the low-metallicity condition (e.g., Hirashita & Ferrara 2002; Cazaux & Spaans 2009). Dust is also an important coolant in star formation, inducing a fragmentation into low-mass stars (Omukai et al. 2005; Schneider et al. 2006). Thus, dust grains are strongly related to the star formation in galaxies. Also, dust grains govern the scattering and absorption (i.e., extinction) of stellar light, in particular, at short wavelengths like ultraviolet (UV), and re-emit in infrared (IR). Consequently, dust grains affect the spectral energy distribution (SED) of galaxies significantly (e.g., Takagi et al. 2003).

The extinction curve, which represents the wavelength dependence of dust extinction, is used to relate the intrinsic stellar SED with the observed SED affected by dust extinction. Thus, the extinction curve is the fundamental tool in interpreting the observational SED of galaxies. Since the extinction curve depends strongly on the physical and optical properties of dust grains (grain size, dust components, etc.) [e.g., Mathis, Rumpl & Nordsieck 1977 (hereafter MRN); Weingartner & Draine 2001; Nozawa & Fukugita 2013], it is important to understand those properties.

The mean extinction curve of the Milky Way (hereafter MW extinction curve) is observationally well investigated (e.g., Fitzpatrick & Massa 2007), and is widely adopted as a template extinction curve in various studies (e.g., Buat et al. 1999; Matsuoka et al. 2005; Kobayashi et al. 2013; Krühler et al. 2013). The MW extinction curve has a bump at 2175 Å which is thought to be generated by small carbonaceous grains and/or polycyclic aromatic hydrocarbons (PAHs) (e.g., Barbaro et al. 2001; Draine 2009a), and shows a steep rise to the far-UV wavelength (called UV slope). By fitting the MW extinction curve, MRN derived the grain size distribution in the Milky Way, $f(a)\mathrm{d}a \propto a^{-3.5}\mathrm{d}a$ with $a = 0.005$–0.25 μm, where a is the grain radius and $f(a)\mathrm{d}a$ is the number density of grains in size interval $[a, a + \mathrm{d}a]$. Furthermore, Weingartner & Draine (2001) performed a detailed fit to the MW extinction curve, finding that the size distributions of carbonaceous and silicate dust grains are quite different from each other unlike MRN. The extinction curves depend on the line of sight, and Cardelli et al. (1989) suggested that the variation of the extinction curves are described by adopting the parameter $R_V \equiv A_V/E(B-V)$, where A_V is the magnitude of the extinction in the V band and $E(B-V)$ is the reddening ($A_B - A_V$, where A_B is the extinction in the B band). Recently, Nozawa & Fukugita (2013) investigated the possible variety of dust properties based on the diversity of the extinction curves observed in the Milky Way.

⋆ E-mail: asano.ryosuke@g.mbox.nagoya-u.ac.jp
† Fellow of the Japan Society for the Promotion of Science (JSPS).

They found that the power-law index and maximum radius of the grain size distribution are tightly constrained to be -3.5 ± 0.2 and 0.25 ± 0.05 μm, respectively. Pei (1992) extended the graphite-silicate grain model which can fit the MW extinction curve (MRN) to the Large and Small Magellanic Clouds (LMC and SMC), and found that the extinction curves in these galaxies can be fitted with the MRN grain size distribution by adjusting only the relative contribution of graphite and silicate.

Many studies have shown that high-z galaxies have different extinction curves from nearby galaxies (e.g., Maiolino et al. 2004; Liang & Li 2009; Gallerani et al. 2010; Hjorth et al. 2013). The extinction curve of the quasar SDSS104845.05+463718.3 (hereafter SDSS1048+4637) at redshift $z = 6.2$ shows the lack of the 2175 Å bump, and is relatively flat at $\lambda \gtrsim 1700$ Å and rising toward shorter wavelengths at $\lambda \lesssim 1700$ Å. Maiolino et al. (2004), by using the model in Todini & Ferrara (2001), showed that the extinction curve is consistent with the dust formation in Type II supernovae (SNe II). Because of their short lifetime (typically 10^{6-7} yr), SNe II are thought to be the origin of dust in high-z Universe. On the other hand, because of the long lifetime of progenitors, asymptotic giant branch (AGB) stars can be dominant sources of dust in galaxies at age $t > 1$ Gyr (but see Valiante et al. 2009). Furthermore, Hirashita et al. (2010) examined the extinction curves in starburst galaxies taking into account not only dust grains produced by SNe II but also the effect of shattering (grain–grain collision) in the warm ionized medium (WIM). They showed that the shattering can lead to the steepness of the extinction curve at UV wavelengths, and indicated that shattering may occur effectively in SDSS1048+4637. Liang & Li (2009) showed that the extinction curves of high-z gamma-ray bursts (GRBs) are different from those of the Milky Way and LMC. Among them, one at $z = 6.3$ appears to have the 2175 Å feature, indicating a difference from SDSS1048+4637. In order to reveal the origin of the differences in the extinction curves among galaxies at high and low-z Universe, it is necessary to clarify the processes that govern the evolution of dust grains in galaxies.

An MRN-like power-law grain size distribution can be realized if the grains are processed by the grain–grain collisions (shattering and coagulation) (e.g., Tanaka, Inaba, & Nakazawa 1996; Kobayashi et al. 2010). Thus, it is probable that the grain–grain collisions are an important process in the Milky Way and perhaps in nearby galaxies in general. In addition, if the metallicity in galaxies is larger than a certain value, the accretion of gas-phase metals on the surface of pre-existing grains (referred to as 'grain growth' in this paper) occurs effectively (Inoue 2011; Asano et al. 2013a). Since grain growth has a potential to change the grain size distribution [e.g., Hirashita & Kuo 2011; Asano et al. 2013b (hereafter A13)], the shape of extinction curves may change by grain growth. In fact, Hirashita (2012) showed that the UV slope on extinction curves becomes steeper by grain growth if the grain size distribution is initially similar to the MRN size distribution.

Various kinds of processes have different effects on different grain sizes. Grains ejected by SNe II into the ISM are relatively large ($a \gtrsim 0.01$ μm) due to the destruction of small grains by the sputtering in reverse shocks (e.g., Bianchi & Schneider 2007; Nozawa et al. 2007). Grains produced in AGB stars may have typical radii ~ 0.1 μm (e.g., Winters et al. 1997; Ventura et al. 2012a,b; Di Criscienzo et al. 2013) and could be described by a log-normal distribution with a peak at $a \sim 0.1$ μm (Yasuda & Kozasa 2012). Further, small grains ($a < 0.01$ μm) are efficiently destroyed by sputtering in interstellar shocks driven by SNe (Nozawa et al. 2006). When grain growth occurs in the interstellar medium (ISM), smaller grains grow more efficiently (e.g., Hirashita & Kuo 2011; A13) because the timescale of grain growth is proportional to the volume-to-surface ratio of a dust grain. In the diffuse ISM, shattering can occur effectively if grains are dynamically coupled with magnetized interstellar turbulence (e.g., Yan et al. 2004; Hirashita & Yan 2009), in particular, large grains ($a \gtrsim 0.1$ μm) acquire larger velocity dispersions than the shattering threshold velocities. Shattering occurs also in SN shocks (e.g., Jones, Tielens & Hollenbach 1996). In dense and cold regions, coagulation of small grains can occur (e.g., Hirashita & Yan 2009; Ormel et al. 2009); consequently, the grain size distribution shifts towards larger sizes (e.g., Hirashita & Li 2013). After all, the above various processes affecting grain size distribution (referred to as 'dust processes' in this paper) occur in a way dependent on the metallicity, total dust amount, and grain size distribution, and could be interrelated. Thus, it is mandatory to construct a model by taking into account all dust processes in a unified framework.

There are some studies on the evolution of the grain size distribution in galaxies (e.g., Liffman & Clayton 1989; O'Donnell & Mathis 1997; Hirashita et al. 2010; Yamasawa et al. 2011). However, they did not consider all the dust processes to simplify their models. Recently, A13 have discussed the evolution of the grain size distribution, taking into account all the dust processes based on chemical evolution of galaxies. A13 showed that the grain size distribution drastically changes with the galactic age because the dominant dust process changes (see Section 2). In view of the discussion in A13, it is expected that the extinction curve also changes with the galactic age due to the change of the dominant dust processes. Therefore, in this paper, we examine the evolution of extinction curves in galaxies using the dust evolution model developed by A13, and check whether we can reproduce the MW extinction curve.

This paper is organized as follows. First, we briefly review the dust evolution model constructed by A13 and explain the theoretical treatment of the extinction curve in Section 2. In Section 3, we show the contributions of various dust processes to the extinction curve. We discuss how we can reproduce the MW extinction curve and the contribution of different grain species in Section 4. We present the conclusions of this paper in Section 5.

2 MODEL

In this section, we first review our dust evolution model for calculating the evolution of the grain size distribution in a galaxy (A13). Then, we explain the method of calculating the extinction at wavelength λ, A_λ (in units of magnitude) based on the grain size distribution calculated.

2.1 Dust evolution model

We briefly introduce the model constructed by A13 and their results. A13 investigated the evolution of the grain size distribution taking into account the dust formation by SNe II and AGB stars, dust destruction by SN shocks in the ISM, grain growth in the cold neutral medium (CNM), grain–grain collisions (shattering and coagulation) in the warm neutral medium (WNM) and CNM. Grain growth in the WNM was not considered because grain growth is more efficient in dense and cold regions (e.g., Liffman & Clayton 1989; Draine 2009a). A13 considered the contribution of the dust processes in the WNM and CNM by introducing the mass fractions of WNM ($\sim$ 6000 K, 0.3 cm^{-3}) and CNM ($\sim$ 100 K,

30 cm^{-3}), $\eta_{\rm WNM}$ and $\eta_{\rm CNM}$, respectively. The sum of $\eta_{\rm WNM}$ and $\eta_{\rm CNM}$ was assumed to be unity in A13 since an equilibrium state of two thermally stable phases (WNM and CNM) is established in the ISM if we consider temperatures less than 10^4 K in the ISM (Wolfire et al. 2003). The grain velocities in the two ISM phases derived by Yan et al. (2004) were adopted to calculate shattering and coagulation.

We assume two dust species, graphite and silicate (Draine & Lee 1984) in the same way as in A13. Although A13 considered a variety of dust species (C, Si, SiO_2, SiC, Fe, FeS, Al_2O_3, MgO, $MgSiO_3$, Mg_2SiO_4 and Fe_2SiO_4; Nozawa et al. 2007; Zhukovska, Gail, & Trieloff 2008) for stellar dust production, carbonaceous dust and all the other dust species are categorized as graphite and silicate [we adopt astronomical silicate, $Mg_{1.1}Fe_{0.9}SiO_4$ (Draine & Lee 1984)], respectively to avoid chemical complexity in grain growth, shattering, and coagulation. A13 examined the contribution of grain growth, shattering and coagulation for two dust species separately. While the complexity of dust species may affect the extinction curves (e.g., Nozawa & Fukugita 2013), the aim of this paper is not a detailed fit to a specific extinction curve but an investigation of the response of extinction curves to the evolution of grain size distribution. Further, it is thought that these two dust species are the main components of dust grains in the Milky Way (Draine & Lee 1984), and Sofia & Meyer (2001) suggested that (Fe+Mg):Si ratio in dust grains is close to 2:1. Thus, the above grain composition is a reasonable approximation. Other possible dust species are discussed in Section 4. We assume that grains are spherical, and that shattering/coagulation occurs if the relative velocity of collisional grains is more/less than the threshold velocity (e.g., Yan et al. 2004; Hirashita & Yan 2009). The threshold velocity of shattering, $v_{\rm shat}$, is assumed to be 1.2 and 2.7 $\mathrm{km\ s^{-1}}$ for carbonaceous dust and silicate dust, respectively (Jones, Tielens & Hollenbach 1996). For the threshold velocity of coagulation, we calculate in the same way as Hirashita & Yan (2009), and the threshold velocity is about 10^{-3}–10^{-1} $\mathrm{km\ s^{-1}}$ depending on the grain size (Chokshi, Tielens, & Hollenbach 1993). Note that if the radius of the shattered fragments is less than 3 Å, we remove the fragments unlike A13.

For the dust evolution model, A13 assumed that the total baryon mass (the sum of the stellar mass and the ISM mass in the galaxy) is constant (closed-box model), and formulated the star formation rate (SFR) by introducing the star formation timescale, $\tau_{\rm SF}$: $\mathrm{SFR}(t) = M_{\rm ISM}(t)/\tau_{\rm SF}$, where $M_{\rm ISM}$ is the ISM mass and t is the galaxy age.

Figure 1 shows the evolution of the grain size distribution (the sum of silicate and carbonaceous dust is shown) with all dust processes considered for $\tau_{\rm SF} = 5$ Gyr. We find that while the grain size distribution is dominated by large grains ($a \gtrsim 0.1$ μm) produced by stars at < 0.1 Gyr, as the galaxy evolution proceeds, the grain size distribution begins to be regulated by the processes in the ISM. In particular, once shattering occurs effectively, a large amount of small grains ($a \lesssim 0.01$ μm) are produced by the fragmentation due to collisions between large grains. The effect of shattering is seen in the increase of small grains at 0.1–1 Gyr. Due to a large amount of small grains, grain growth occurs effectively because the surface-to-volume ratio of smaller grains is larger than that of larger grains. Consequently, the bump at $a \sim 0.01$ μm emerges at 1–10 Gyr. Smaller grains can acquire lower velocity dispersions since they are coupled with smaller scale turbulence (e.g., Yan et al. 2004). Therefore, after small grains are enhanced, the coagulation mainly occurs by collisions between small grains whose velocity dispersions are smaller than the coagulation threshold. The shift of the bump position from 1 to 10 Gyr is due to coagulation. For further details and parameter dependences of grain size distribution, see A13.

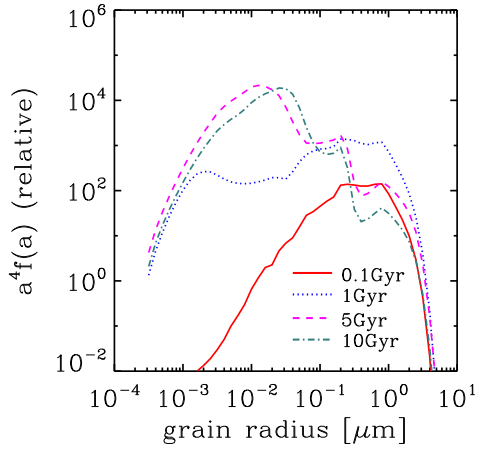

Figure 1. Example of the evolution of the grain size distribution. Solid, dotted, dashed, and dot–dashed lines represent the cases at $t = 0.1, 1, 5, 10$ Gyr, respectively, with $\tau_{\rm SF} = 5$ Gyr. The mass fractions, $\eta_{\rm WNM}$ and $\eta_{\rm CNM}$, are set to be 0.5.

2.2 Extinction curve

Extinction curves are powerful tools to examine the dust properties in galaxies. In order to analyze extinction curves, the optical constants for each dust species are necessary. In this paper, we adopt the optical constants derived by Draine & Lee (1984) to calculate the grain extinction cross section normalized to the geometrical cross section πa^2 as a function of wavelength and grain radius, $Q_{\rm ext,X}(\lambda, a)$, where the subscript X represents grain species (X = carbonaceous dust or silicate dust) and λ is the wavelength.

The optical depth of dust species X at a given wavelength λ, $\tau_{\rm X,\lambda}$, is defined as

$$\tau_{\rm X,\lambda} = \int_0^\infty \pi a^2 C Q_{\rm ext,X}(\lambda, a) f_{\rm X}(a) {\rm d}a, \tag{1}$$

where C is a normalization constant and $f_{\rm X}(a)$ is defined so that $f_{\rm X}{\rm d}a$ is the number density of species X with radii in the range $[a, a + {\rm d}a]$. The extinction in units of magnitude is proportional to the optical depth, and is expressed as

$$A_{\rm X,\lambda} = 1.086 \tau_{\rm X,\lambda}, \tag{2}$$

where $A_{\rm X,\lambda}$ is the extinction of dust species X in units of magnitude at wavelength λ. The total extinction in units of magnitude, A_λ, is expressed as

$$A_\lambda = \sum_{\rm X} A_{\rm X,\lambda}. \tag{3}$$

In this work, we consider the extinction curve normalized to the V band value, $A_\lambda / A_{\lambda_V}$, so C and factor 1.086 cancel out.

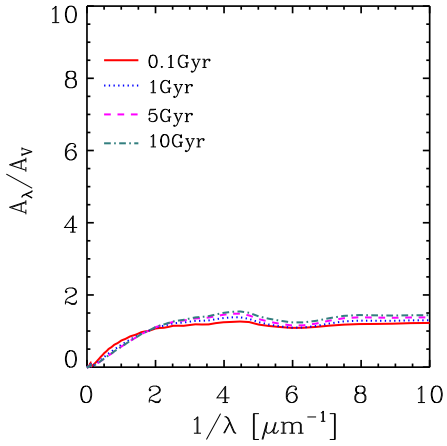

Figure 2. Evolution of extinction curves with the dust formation by SNe II and AGB stars. Solid, dotted, dashed, and dot–dashed lines represent the cases at $t = 0.1, 1, 5, 10$ Gyr, respectively, with $\tau_{\rm SF} = 5$ Gyr.

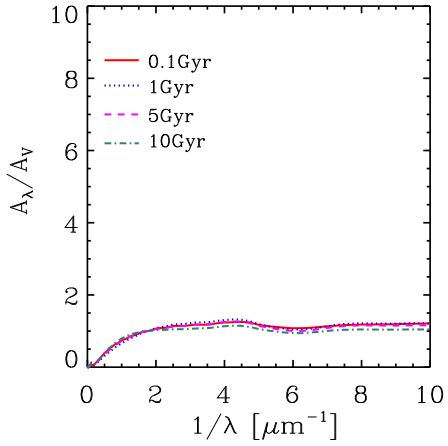

Figure 3. Same as Fig. 2 but with the dust destruction by SN shocks in the ISM in addition.

3 RESULTS

In this section, we show the effects of each dust process on the extinction curve; we add the following processes one by one, the dust formation by SNe II and AGB stars, dust destruction by SN shocks in the ISM, grain growth in the ISM, shattering and coagulation in the ISM. The loss of dust by astration is always included, although it does not affect the shape of extinction curve. We adopt star formation timescale $\tau_{\rm SF} = 5$ Gyr, and the mass fraction of the WNM and CNM $\eta_{\rm WNM} = \eta_{\rm CNM} = 0.5$ unless otherwise stated.

3.1 Dust formation by SNe II and AGB stars

In Fig. 2, we show the evolution of the extinction curves with the dust formation by SNe II and AGB stars. From Fig. 2, we observe that the extinction curves are flat throughout any galactic ages, and do not change significantly with time. This is because the size distribution of grains produced by SNe II and AGB stars is dominated by large grains ($a \gtrsim 0.1$ μm) (Nozawa et al. 2007; Yasuda & Kozasa 2012) and does not change with galactic ages considerably (Fig. 1 of A13).

A13 showed that although the size distribution of grains produced by SNe II depends on the hydrogen number density of the ISM surrounding the SNe II, $n_{\rm SN}$ (we adopt $n_{\rm SN} = 1.0$ cm^{-3} in this paper), the tendency that the grain size distribution is dominated by large grains is unchanged.

3.2 Dust destruction

In Fig. 3, we show the evolution of extinction curve with the dust destruction by SN shocks in the ISM in addition to the dust formation by stars. The timescale on which the dust destruction affects the grain size distribution in galaxies, $\tau_{\rm SN}$, is about $\tau_{\rm SN} \sim 0.1\tau_{\rm SF}$ (A13). Thus, we can not observe the difference between the extinction curves with and without dust destruction at 0.1 Gyr (solid lines in Fig. 2 and Fig. 3). The extinction curves with dust destruction are slightly flatter than those produced by stardust (see Fig. 2) at $t \gtrsim 1$ Gyr. Since smaller grains are more easily destroyed by SN shocks (Nozawa et al. 2006; Yamasawa et al. 2011; A13), the extinction curves become flatter than the case without dust destruction by SN shocks in the ISM (Fig. 2).

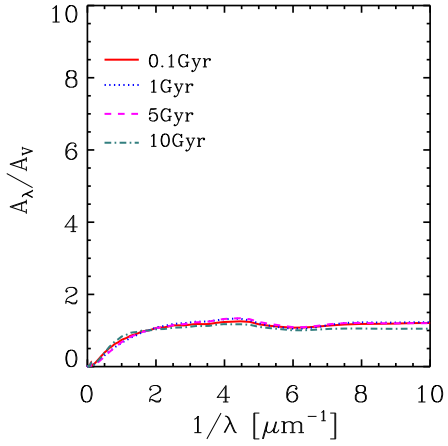

Figure 4. Same as Fig. 3 but with grain growth in addition. We adopt $\eta_{\rm CNM} = 0.5$.

A13 examined the effect of dust destruction by SN shocks in the ISM for various $n_{\rm SN}$, and showed that the effect is larger for larger $n_{\rm SN}$. Thus, the extinction curve becomes flatter in the case with larger $n_{\rm SN}$.

3.3 Grain growth

Figure 4 shows the evolution of extinction curves with the dust formation by SNe II and AGB stars, dust destruction by SN shocks in the ISM and grain growth in the CNM. We find that the extinction curves are almost the same as in Fig. 3. In this case, since the total surface area of grains is dominated by large grains with $a > 0.3$ μm (A13), the effect of grain growth is prominent at large sizes ($a \gtrsim 0.1$ μm). Since the grains are already large, grain growth just keeps the extinction curve flat.

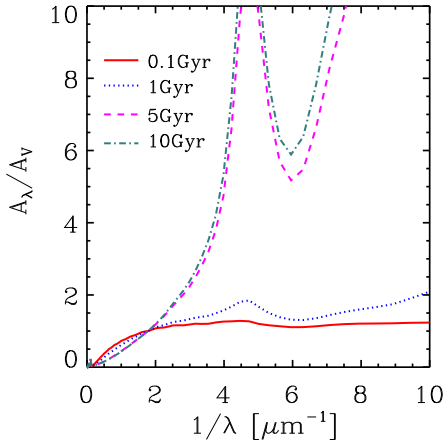

Figure 5. Same as Fig. 4 but with shattering in addition. We adopt $\eta_{\rm WNM} = \eta_{\rm CNM} = 0.5$.

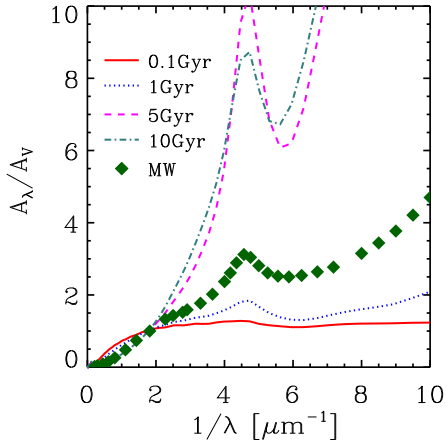

Figure 6. Same as Fig. 5 but with coagulation in addition. Filled diamonds represent the extinction curve of the Milky Way (Whittet 2003).

3.4 Shattering

We show the evolution of extinction curve with shattering in addition to all the dust processes considered in Section 3.3. From Fig. 5, we observe that the extinction curve is almost flat until galactic age $t \sim 1$ Gyr; at $t \lesssim 1$ Gyr, shattering is ineffective due to the small dust abundance, and the grain size distribution is similar to the case without shattering (A13). A13 discussed the timescale on which the grain size distribution changes due to the processes in the ISM (especially shattering), and obtained the timescale $\tau_{\rm shat} \sim 1\ (\tau_{\rm SF}/{\rm Gyr})^{1/2}$ Gyr from a rough order-of-magnitude estimate (see their Appendix B). Thus, there is only a small difference between the cases with and without shattering at $t < 1$ Gyr for $\tau_{\rm SF} = 5$ Gyr. At $t = 5$ Gyr, the extinction curve drastically changes and starts to have a prominent bump at $1/\lambda \sim 4.5\ \mu{\rm m}^{-1}$ (the so-called 2175 Å bump) and a steep slope toward shorter wavelengths. This is because the grain size distribution changes considerably due to the interplay between grain growth and shattering (A13). A13 showed that once shattering occurs effectively, the number of small grains increases with the decrease in the number of large grains. Thus, the total surface area of grains per grain mass becomes large, and grain growth occurs effectively especially at small grain radii ($\lesssim 0.01\ \mu$m), forming a bump at $a \sim 0.01\ \mu$m in the grain size distribution. Consequently, the 2175 Å bump and UV slope on the extinction curve become larger and steeper, respectively. In fact, Hirashita (2012) also showed that the 2175 Å bump and the UV slope are enhanced by grain growth. At $t = 10$ Gyr, although grain growth becomes ineffective due to the large depletion of heavy elements (e.g., Asano et al. 2013a), the abundance of small grains still increases by shattering. Consequently, the 2175 Å bump and the UV slope become larger and steeper at 10 Gyr than at 5 Gyr.

3.5 Coagulation

In Fig. 6, we show the evolution of the extinction curve with all the dust processes considered in our model. We find that the extinction curves at $t = 0.1$ and 1 Gyr are flat, and that there is little difference between the extinction curves with and without coagulation (see Fig. 5). As mentioned in Section 2.1, since coagulation occurs when the relative velocity of colliding grains is less than $v_{\rm coag}$ [fiducial $v_{\rm coag} \sim 10^{-3}$–$10^{-1}$ km s^{-1} depending on the grain size (Chokshi, Tielens, & Hollenbach 1993)], coagulation does not occur for large grains ($a \gtrsim 0.1\ \mu$m) whose velocities are above the coagulation threshold. At $t = 5$ and 10 Gyr, the 2175 Å bump is smaller, and the UV slope is flatter than that in the case without coagulation (Fig. 5). A13 showed that the bump at $a \sim 0.01\ \mu$m in the grain size distribution shifts to larger sizes by coagulation, and finally moves to $a \sim 0.03$–$0.05\ \mu$m at 10 Gyr. As the abundance of large grains is increased by coagulation, the bump at $1/\lambda \sim 4.5\ \mu{\rm m}^{-1}$ and the UV slope become smaller and flatter, respectively.

For reference, we show the MW extinction curve taken from Whittet (2003). From Fig. 6, we find that our calculated extinction curve at the age of the Milky Way (~ 10 Gyr) is steeper and has a larger 2175 Å bump than the extinction curve of the Milky Way. The main aim of this paper is not to reproduce the MW extinction curve precisely but to examine the trend of evolution of the extinction curve. Nevertheless, we will propose and examine some possibilities of reproducing the MW extinction curve by slightly modifying our model in Section 4.1.

3.6 Parameter dependence

So far, we have adopted star formation timescale $\tau_{\rm SF} = 5$ Gyr, mass fractions of WNM and CNM $\eta_{\rm WNM} = \eta_{\rm CNM} = 0.5$ as a fiducial case. Here, we demonstrate how the extinction curve depends on these parameters.

In panels (a) and (b) of Fig. 7, we show the time evolution of the extinction curve in the cases with $\tau_{\rm SF} = 0.5$ and 50 Gyr, respectively, for $\eta_{\rm WNM} = \eta_{\rm CNM} = 0.5$. Focusing on panel (a), we find that the extinction curve at 1 Gyr is different from that in Fig. 6 where $\tau_{\rm SF} = 5$ Gyr is adopted. If $\tau_{\rm SF}$ is short, the total dust amount ejected by stars is large at younger galactic ages. This early increase in dust abundance shortens the timescale on which shattering becomes effective according to $\tau_{\rm shat} \sim 1(\tau_{\rm SF}/{\rm Gyr})^{1/2}$ Gyr (A13; Section 3.4). Thus, shattering is already able to produce a large amount of small grains at < 1 Gyr for $\tau_{\rm SF} = 0.5$ Gyr. Consequently, the extinction curve has the 2175 Å bump and steep UV slope at earlier phases of galaxy evolution. We also observe that the extinction curves at $t = 5$ and 10 Gyr are almost identical

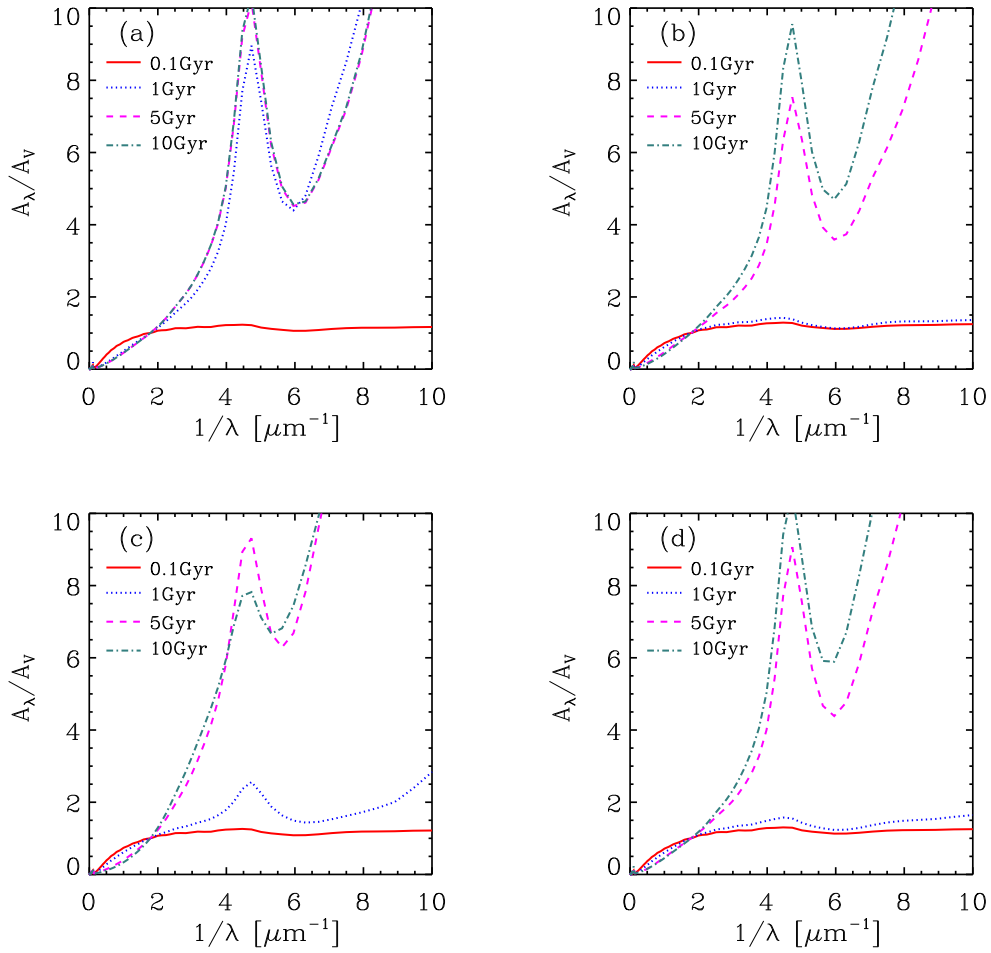

Figure 7. Same as Fig. 6 but with (a) $\tau_{\rm SF} = 0.5$ Gyr and $\eta_{\rm WNM} = \eta_{\rm CNM} = 0.5$, (b) $\tau_{\rm SF} = 50$ Gyr and $\eta_{\rm WNM} = \eta_{\rm CNM} = 0.5$, (c) $\tau_{\rm SF} = 5$ Gyr, $\eta_{\rm WNM} = 0.1$ and $\eta_{\rm CNM} = 0.9$ and (d) $\tau_{\rm SF} = 5$ Gyr, $\eta_{\rm WNM} = 0.9$ and $\eta_{\rm CNM} = 0.1$.

to each other. This means that the grain size distribution does not change at these ages for $\tau_{\rm SF} = 0.5$ Gyr. Since the total dust amount decreases rapidly by astration in the case with the short star formation timescale (e.g., Asano et al. 2013a), shattering and coagulation become inefficient at those ages. As a result, the shape of grain size distribution does not change significantly. On the other hand, panel (b) shows the result for $\tau_{\rm SF} = 50$ Gyr. We find that the 2175 Å bump continues to grow even after 5 Gyr. This is because the increase of the total dust amount is slower due to the longer star formation timescale than the case in panel (a). Indeed, $\tau_{\rm shat} \sim 7$ Gyr is consistent with the rapid increase of small grains at 5–10 Gyr (see also Fig. 9 in A13). Thus, the timescales of all dust processes we considered become long (e.g., A13), and the evolution of the extinction curve slows down.

Panels (c) and (d) of Fig. 7 show the cases with $(\eta_{\rm WNM}, \eta_{\rm CNM}) = (0.1, 0.9)$ and $(0.9, 0.1)$, respectively, for $\tau_{\rm SF} = 5$ Gyr. Since a large $\eta_{\rm CNM}$ is adopted in panel (c), the timescale of coagulation is short. Consequently, the 2175 Å bump becomes small at earlier phases than the case with a small $\eta_{\rm CNM}$. In panel (d) where a small $\eta_{\rm CNM}$ is adopted, the timescale of grain growth is longer than that for panel (c). As mentioned in section 3.4, the 2175 Å bump becomes prominent due to grain growth. Thus, the 2175 Å bump becomes more prominent at later phases than in the case with a larger $\eta_{\rm CNM}$.

4 DISCUSSION

4.1 Reproducing the MW extinction curve

In the previous section, we showed the evolution of the extinction curve in galaxies taking into account various dust processes. We found that since stellar dust is biased to large grains ($a \gtrsim 0.1$ μm), the extinction curve at the earliest stage of galaxy evolution is flat. After $t \sim \tau_{\rm shat} \sim 1\ (\tau_{\rm SF}/{\rm Gyr})^{1/2}$ Gyr, shattering and grain growth occur effectively, and the extinction curve becomes steeper and has a larger bump at $1/\lambda \sim 4.5$ $\mu{\rm m}^{-1}$ than that of the MW extinction curve. After coagulation becomes effective, the bump becomes small. However, compared with the MW extinction curve, the calculated extinction curves are too steep and have too large a bump. The reason for this is too abundant small grains, forming the bump at $a \sim 0.01$ μm in the grain size distribution (Fig. 1). Thus, it is crucial to weaken this bump in order to reproduce the MW extinction curve. As explained in Section 3.4, the bump in the grain size distribution is formed by grain growth. This means that our models may have overestimated grain growth. Thus, as the first

possibility of reproducing the MW extinction curve, we examine a model in which only grain growth is tuned off. This is referred to as (i) no grain growth model.

There is another way of weakening the bump in the grain size distribution. In the current model, coagulation takes place only for the grains with radii less than ~ 0.05 μm because large grains have larger velocities than the coagulation threshold (Section 3.5). However, if the grains can coagulate beyond 0.05 μm, the bump in the grain size distribution could be smoothed out. There are some indications that the grains could coagulate beyond 0.05 μm: Ossenkopf (1993) argued that fluffy grains can be formed in dense regions by coagulation. Fluffiness enhances the cross-section in grain–grain collision, raising the coagulation rate. Fluffy grains can also absorb collision energy, raising the coagulation threshold (e.g., Ormel et al. 2009). Enhancement of coagulation efficiency is also suggested by Hirashita & Li (2013) to explain μm–sized grains in dense molecular cloud cores. Thus, to investigate the possibility of strong coagulation, we examine a model in which we do not apply any coagulation threshold velocity. This model is referred to as (ii) strong coagulation model.

Figure 8 shows the extinction curves and the grain size distributions for carbon and silicate dust at the galactic age 10 Gyr for the (i) no grain growth model and (ii) strong coagulation model. We adopt $\tau_{\rm SF} = 5$ Gyr, $\eta_{\rm WNM} = \eta_{\rm CNM} = 0.5$. For comparison, we show the grain size distribution using the same parameters as in section 3.5 for a fiducial case. In both panels, we find that the MW extinction curve is better reproduced than the cases considered in Section 3. For the no grain growth model [panel (i)], we observe that the calculated extinction curve is similar to that of the Milky Way since the shape of the grain size distribution is similar to the MRN distribution. This is because when grain growth is not considered, the bump produced at $a < 0.01$ μm in the size distribution (see Fig. 1) cannot be formed. Consequently, the grain size distribution approaches a power-law size distribution with a power index ~ -3.5 because shattering and coagulation are dominant processes to form the grain size distribution (e.g., Kobayashi et al. 2010). However, if we do not consider the contribution of grain growth to the evolution of the total dust mass in galaxies, it is hard to reproduce the total dust mass of the Milky Way as has been pointed out by e.g., Zhukovska, Gail, & Trieloff (2008); Draine (2009a); Inoue (2011); Asano et al. (2013a). For example, Inoue (2011) showed that in the case without grain growth, the total dust amount in a galaxy is about ten times less than that in the Milky Way even if dust grains are not destroyed by SN shocks. Thus, by this scenario, we can obtain the extinction curve similar to that of the Milky Way, but has difficulty in reproducing the total dust mass.

Next, we discuss the extinction curve for the case of strong coagulation [panel (ii)]. We observe that the extinction curve has a slightly larger bump and a steeper UV slope than the MW extinction curve, since the abundance of small grains ($a < 0.01$ μm) is slightly enhanced compared with the MRN size distribution. However, we can find that the bump in the grain size distribution disappears. In this model, we remove the coagulation threshold, so the bump in the grain size distribution can shift toward larger sizes than the fiducial case. When the radii of grains reach at ~ 0.2 μm, the grains are shattered effectively, and consequently, the bump is vanished. Furthermore, thanks to the supply of large grains by strong coagulation, shattering is induced, and as a result, the small grains are supplied. Hence, the amount of the small grains is larger than the fiducial case. With such an interplay, the size distribution is expected to approach the power-law size distribution with a power index -3.5 (Tanaka, Inaba, & Nakazawa 1996; Kobayashi et al. 2010). Consequently, the extinction curve is nearer to the MW extinction curve than the cases in Section 3. In addition, unlike the case (i), the case (ii) may naturally account for the evolutions of the total dust mass, grain size distribution and extinction curve in a galaxy at the same time. Note that power-law-like grain size distributions can also reproduce the LMC and SMC extinction curves (Pei 1992). Thus, we conclude that the strong interplay of shattering and coagulation is important to reproduce extinction curves observed in nearby galaxies.

4.2 Other possible grain species

As we mentioned in Section 1, we do not consider PAHs in this work. PAHs are important in reproducing the SEDs at near- and mid- infrared wavelengths in galaxies (e.g., Li & Draine 2001), and PAHs may contribute to the 2175 Å bump in the MW extinction curve (e.g., Weingartner & Draine 2001). However, what kind of grains dominate the bump at 2175 Å is still a matter of debate (e.g., Draine & Malhotra 1993; Li & Draine 2001; Draine 2003). Furthermore, although carbon-rich AGB stars or shattering process in grain–grain collisions are considered as possible sources of PAHs (e.g., Latter 1991; Jones, Tielens & Hollenbach 1996; Seok, Hirashita, & Asano 2013), the main formation mechanism of PAHs is still controversial.

We do not consider other carbonaceous dust, such as glassy carbon or amorphous carbon. Nozawa & Fukugita (2013) discussed the effect of these species on the extinction curves, and showed that they make the bump at 2175 Å small. This means that the 2175 Å bump which we calculated may be overestimated. Recently, Jones et al. (2013) have constructed a dust model considering hydrogenated amorphous carbon without graphite, and the model reproduced the extinction curve, IR extinction, IR-mm dust emission, and albedo of the Milky Way. In fact, their best fitting model also depends on the dust properties adopted. However, the trend that the small carbonaceous grains produce the 2175 Å bump and large grains show the flat extinction does not change. Thus, the evolutionary trend of the shape of extinction curves would not change significantly even if species other than graphite are adopted as a representative carbonaceous species.

In this paper, we consider the astronomical silicate as one of the main dust species. However, many observations have suggested that other species of cosmic silicate may exist as iron-poor ones such as enstatite ($MgSiO_3$) and forsterite (Mg_2SiO_4) (e.g., Draine 2003). In addition, many of the iron atoms are likely to be locked up in pure Fe grains (Draine 2009b) and other Fe-bearing grains such as magnetite (Fe_3O_4) and iron sulfide (FeS) (e.g., Cowie & Songaila 1985). Recently, Nozawa & Fukugita (2013) showed that the extinction curve produced by Fe or Fe_3O_4 or FeS grains in addition to the combination of graphite and Mg_2SiO_4 is similar to that led by the combination of graphite and astronomical silicate, as long as most of Mg, Si, and Fe atoms are locked up in these grains. This indicates that the astronomical silicate and the combination of other dust species have similar optical properties to each other. Thus, even if we consider other species of silicate grains, it is unlikely that this would largely modify a discrepancy between the modelled and MW extinction curves.

4.3 Remarks on extinction in high-z galaxies

In Section 4.1, we compared our models with the MW extinction curve, and investigated what the important physics that reproduce

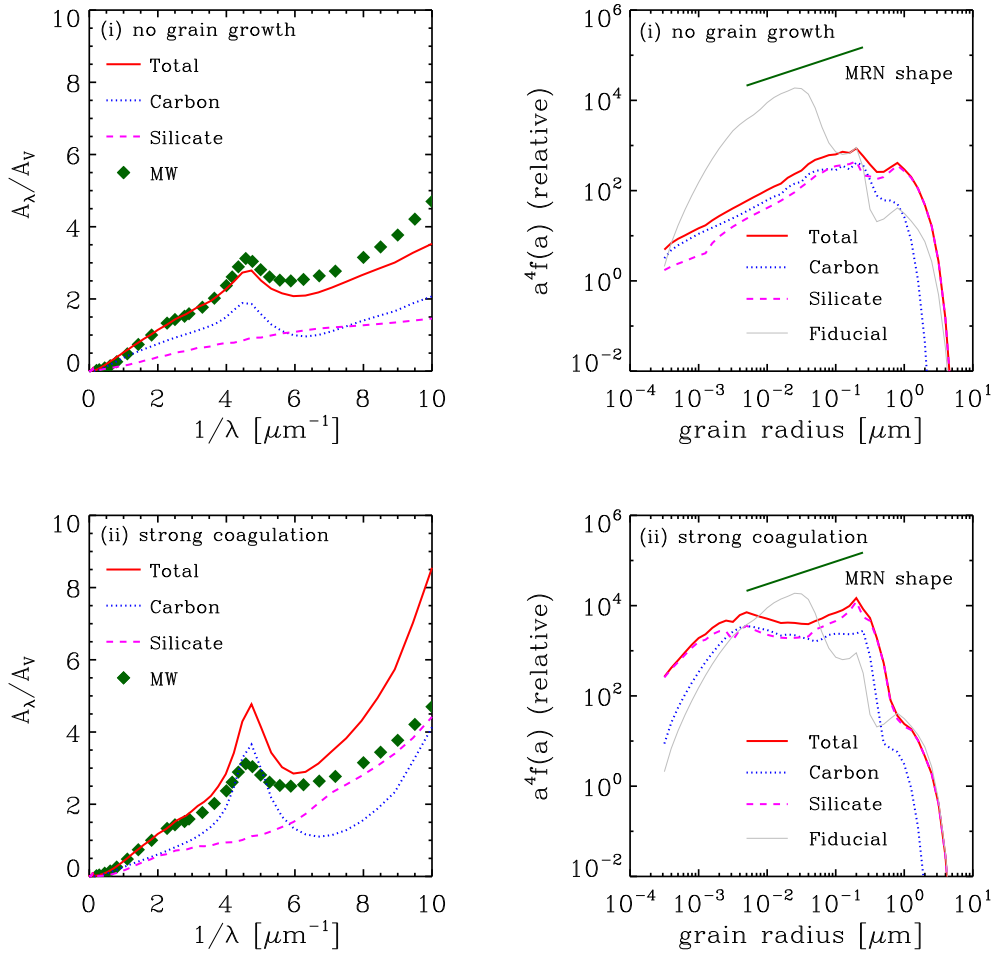

Figure 8. Extinction curves (left panels) and grain size distributions (right panels) at galactic age 10 Gyr for total grains (solid line), carbon dust (dotted line) and silicate dust (dashed line). From top to bottom, two panels represent for the cases (i) without grain growth, and (ii) without coagulation threshold velocity. For reference, we plot the result of grain size distribution using the same parameters in section 3.5 (thin solid line), and the MW extinction curve (filled diamond) (Whittet 2003). We adopt $\tau_{\rm SF} = 5$ Gyr and $\eta_{\rm WNM} = \eta_{\rm CNM} = 0.5$.

the MW extinction curve is. Here, we consider implication of our results for observed extinction curves in high-z galaxies.

Recently, the extinction curves in high-z galaxies have been explored by many authors (e.g., Maiolino et al. 2004; Gallerani et al. 2010; Hjorth et al. 2013). Indeed, from observations, Gallerani et al. (2010) showed that the extinction curves in high-z ($z > 4$) QSOs tend to be flatter than those in nearby galaxies. In addition, these flat extinction curves in high-z galaxies are thought to be dominated by dust grains ejected by SNe II whose lifetime is short (typically 10^{6-7} yr) (e.g., Maiolino et al. 2004; Hirashita et al. 2008). Our result that the extinction curves in the early stage of galaxy evolution are relatively flat, is likely consistent with their results, although our extinction curves may be too flat. However, there is a suggestion that the large dust amount of the dusty QSOs in high-z Universe is regulated by grain growth (e.g., Michałowski et al. 2010; Kuo & Hirashita 2012). This claim is strengthened by the fact that these dusty QSOs in high-z Universe have metallicity $Z > Z_\odot$ (e.g., Juarez et al. 2009). As shown by our calculations, once grain growth occurs, the extinction curve changes significantly. Thus, as we tried in Section 4.1, strong coagulation may be worth considering also for high-z QSOs. However, we should note that QSOs with steep extinction curves may be missed from the sample because of the strong UV (optical in the observer's frame) extinction.

The rest-UV SEDs in high-z galaxies ($z \gtrsim 4$) have been investigated by several authors (e.g., Bouwens et al. 2009; González et al. 2012). In particular, it is reported that UV colors in these galaxies become bluer with increasing redshift (e.g., Bouwens et al. 2009). This fact is generally interpreted as little dust amount in galaxies. However, the relation between extinction and UV color depends on the extinction curve (Wilkins et al. 2013). In particular, the blue color may be explained with a flat extinction curve shown by our results in the early stage of galaxy evolution. Thus, there may be a significant amount of dust even in high-z galaxies with blue colors, which implies that the intrinsic luminosity may be underestimated.

The strong 2175 Å feature in star forming galaxies at $1 < z < 2.5$ (the age of the Universe is $\sim$ 3–6 Gyr in a ΛCDM cosmological model with $\Omega_\Lambda = 0.7$, $\Omega_{\rm M} = 0.3$, and $H_0 = 70$ km s^{-1} Mpc^{-1}) is reported by Noll et al. (2007). They found the robust evidence of the 2175 Å bump in one-third of their sample. The existence of the 2175 Å bump in galaxies at these redshifts supports our re-

sults that the bump becomes strong in galaxies at $t \sim \tau_{\rm shat} \sim 1\ (\tau_{\rm SF}/{\rm Gyr})^{1/2}$ Gyr with $\tau_{\rm SF} \lesssim 10$ Gyr. Thus, shattering and grain growth may be effective in these galaxies, and the variation of the extinction curve can be explained by the difference of the galactic age and the star formation timescale.

5 CONCLUSION

We investigated the evolution of extinction curve in galaxies based on the evolution model of grain size distribution (A13). We took into account various dust processes; dust formation by SNe II and AGB stars, dust reduction through astration, dust destruction by SN shocks in the ISM, grain growth in the CNM, grain–grain collisions (shattering and coagulation) in the WNM and CNM.

We found that the extinction curve is flat in the early stage of galaxy evolution because of large grains ($a \gtrsim 0.1$ μm) produced by stars. As the galaxy evolution proceeds, shattering becomes effective, and the number of small grains increases. Further on, these small grains grow due to grain growth, forming a bump at $a \sim 10^{-3}$–10^{-2} μm in the grain size distribution. Since the relatively small grains are dominant in grain size distribution, the extinction curve has a large bump at $1/\lambda \sim 4.5$ $\mu{\rm m}^{-1}$ and steep UV slope. The timescale on which dust processes in the ISM (grain growth, shattering and coagulation) begin to control the grain size distribution, is estimated as $t \sim 1(\tau_{\rm SF}/{\rm Gyr})^{1/2}$ Gyr. After coagulation occurs effectively, the extinction curves become flatter but still tend to be steeper than the MW extinction curve. We also found that for reproducing the MW extinction curve, it may be important to consider a larger contribution of coagulation than that we have assumed. This means that the strong interplay between shattering and coagulation induced by strong coagulation could be essential to reproduce the MW extinction curve. We conclude that the extinction curves in galaxies drastically changes with galactic age because of the evolution of grain size distribution.

ACKNOWLEDGMENTS

We thank the anonymous referee for her/his helpful comments which improved the quality and clarity of this paper. We are grateful to Takashi Kozasa, Anthony P. Jones, Daisuke Yamasawa, and Asao Habe for fruitful discussions. We thank H. Kobayashi for helpful discussions on the process of the grain–grain collisions and the evolution of the grain size distribution. RSA has been supported from the Grant-in-Aid for JSPS Research under Grant No. 23-5514. TTT has been supported by the Strategic Young Researcher Overseas Visits Program for Accelerating Brain Circulation No. R2405 and the Grant-in-Aid for the Scientific Research Fund (20740105, 23340046) commissioned by the MEXT. HH is supported by NSC grant 102-2119-M-001-006-MY3. TN has been supported by World Premier International Research Center Initiative (WPI Initiative), MEXT, Japan, and by the Grant-in-Aid for Scientific Research of the JSPS (22684004, 23224004).

REFERENCES

Asano, R. S., Takeuchi, T. T., Hirashita, H., & Inoue, A. K. 2013a, Earth Planets and Space, 65, 213
Asano, R. S., Takeuchi, T. T., Hirashita, H., & Nozawa, T. 2013b, MNRAS, 432, 637 (A13)
Barbaro, G., Mazzei, P., Morbidelli, L., Patriarchi, P., & Perinotto, M. 2001, A&A, 365, 157
Bianchi, S., Schneider, R. 2007, MNRAS, 378, 973
Bouwens, R. J., Illingworth, G. D., Franx, M., et al. 2009, ApJ, 705, 936
Buat, V., Donas, J., Milliard, B., & Xu, C. 1999, A&A, 352, 371
Calura, F., Pipino, A., & Matteucci, F. 2008, A&A, 479, 669
Cardelli, J. A., Clayton, G. C., & Mathis, J. S. 1989, ApJ, 345 245
Cazaux, S., & Tielens, A. G. G. M. 2004, ApJ, 604, 222
Cazaux, S., & Spaans, M. 2009, A&A, 496, 365
Chokshi, A., Tielens, A. G. G. M., & Hollenbach, D. 1993, ApJ, 407, 806
Cowie, L. L., & Songaila, A. 1986, ARA&A, 24, 499
Di Criscienzo, M., Dell'Agli, F., Ventura, P., Schneider, R., Valiante, R., La Franca, F., Rossi, C., Gallerani, S., & Maiolino, R. 2013, MNRAS, 433, 313
Draine, B. T. 2003, ARA&A, 41, 241
Draine, B. T. 2009, in Henning Th., Grün E., Steinacker J., eds, Cosmic Dust – Near and Far, ASP Conference Series, ASP, San Francisco, p. 453
Draine, B. T. 2009, SSRv, 143,333
Draine, B. T., & Lee, H. M. 1984, ApJ, 285, 89
Draine, B. T., & Malhotra, S. 1993, ApJ, 414, 632
Fitzpatrick, E. L., & Massa, D. 2007, ApJ, 663, 320
Gallerani, S., Maiolino, R., Juarez, Y., Nagao, T., Marconi, A., Bianchi, S., Schneider, R., Mannucci, F., Oliva, T., Willott, C. J., Jiang, L., & Fan, X. 2010, A&A, 523, 85
González, V., Bouwens, R. J., Labbé, I., Illingworth, G., Oesch, P., Franx, M., & Magee, D. 2012, ApJ, 755, 148
Hirashita, H., & Ferrara, A. 2002, MNRAS, 337, 921
Hirashita, H., Nozawa, T., Takeuchi, T. T., & Kozasa, T. 2008, MNRAS, 384, 1725
Hirashita, H., & Yan, H. 2009, MNRAS, 394, 1061
Hirashita, H., Nozawa, T., Yan, H., & Kozasa, T. 2010, MNRAS, 404, 1448
Hirashita, H. & Kuo, T-M. 2011, MNRAS, 416, 1340
Hirashita, H. 2012, MNRAS, 422, 1263
Hirashita, H., & Li, Z.-Y. 2013, MNRAS, 434, L70
Hjorth, J., Vreeswijk, P. M., Gall, C., & Watson, D. 2013, ApJ, 768, 173
Inoue, A. K. 2011, Earth Planets and Space, 63, 1
Jones, A. P., Tielens, A. G. G. M., Hollenbach, D. J. 1996, ApJ, 469, 740
Jones, A. P., Fanciullo, L., Köhler, M., Verstraete, L., and Guillet, V., Bocchio, M., & Ysard, N. 2013, A&A, 558, A62
Juarez, Y., Maiolino, R., Mujica, R., Pedani, M., Marinoni, S., Nagao, T., Marconi, A., & Oliva, E. 2009, A&A, 494, L25
Kobayashi, H., Tanaka, H., Krivov, A. V., Inaba, S. 2010, Icarus, 209, 836
Kobayashi, M. A. R., Inoue, Y., & Inoue, A. K. 2013, ApJ, 763, 3
Kuo, T-M., & Hirashita, H. 2012, MNRAS, 424, L34
Krühler, T. et al. 2013, A&A, 557, 18
Latter, W. B. 1991, ApJ, 377, 187
Li, A., & Draine, B. T. 2001, ApJ, 554, 778
Liang, S. L., & Li, A. 2009, ApJ, 690, L56
Liffman, K., & Clayton, D. D. 1989, ApJ, 340, 853
Maiolino, R., Schneider, R., Oliva, E., Bianchi, S., Ferrara, A., Mannucci, F., Pedani, M., & Roca Sogorb, M. 2004, Nat, 431, 533
Mathis, J. S., Rumpl, W., & Nordsieck, K. H. 1977, ApJ, 217, 425 (MRN)

Matsuoka, Y., Oyabu, S., Tsuzuki, Y., Kawara, K., & Yoshii, Y. 2005, PASJ, 57, 563
Michałowski, M. J., Murphy, E. J., Hjorth, J., Watson, D., Gall, C., & Dunlop, J. S. 2010, A&A, 522, A15
Noll, S., Pierini, D., Pannella, M., & Savaglio, S. 2007, A&A, 472, 455
Nozawa, T., Kozasa, T., & Habe, A. 2006, ApJ, 648, 435
Nozawa, T., Kozasa, T., Habe, A., Dwek, E., Umeda, H., Tominaga, N., Maeda, K., & Nomoto, K. 2007, ApJ, 666, 955
Nozawa, T., & Fukugita, M. 2013, ApJ, 770, 27
O'Donnell, J. E., & Mathis, J. S. 1997, ApJ, 479, 806
Omukai, K., Tsuribe, T., Schneider, R., & Ferrara, A. 2005, ApJ, 626, 6270
Ormel, C. W., Paszun, D., Dominik, C., & Tielens, A. G. G. M. 2009, A&A, 502, 845
Ossenkopf, V. 1993, A&A, 280, 617
Pei, Y. C. 1992, ApJ, 395, 130
Schneider, R., Omukai, K., Inoue, A. K., & Ferrara, A. 2006, MNRAS, 369, 1437
Schmidt, M. 1959, ApJ, 129, 243
Seok, J. Y., Hirashita, H., & Asano, R. S. 2013, MNRAS, submitted
Sofia, U. J., & Meyer, D. M. 2001, ApJL, 554, L221
Takagi, T., Vansevičius, V., & Arimoto, N. 2003, PASJ, 55, 385
Tanaka, H., Inaba, S., & Nakazawa, K. 1996, Icarus, 123, 450
Todini, P., & Ferara, A. 2001, MNRAS, 325, 726
Valiante, R., Schneider, R., Bianchi, S., Andersen, A. C. 2009, MNRAS, 397, 1661
Ventura, P., di Criscienzo, M., Schneider, R., Carini, R., Valiante, R., D'Antona, F., Gallerani, S., Maiolino, R., & Tornambé, A. 2012a, MNRAS, 420, 1442
Ventura, P., di Criscienzo, M., Schneider, R., Carini, R., Valiante, R., D'Antona, F., Gallerani, S., Maiolino, R., & Tornambé, A. 2012b, MNRAS, 424, 2345
Weingartner, J. C., & Draine, B. T. 2001, ApJ, 548, 296
Whittet, D. C. B. 2003, Dust in the Galactic Environment, 2nd ed, p. 76, IoP Publishing, Bristol and Philadelphia
Wilkins, S. M., Bunker, A., Coulton, W., Croft, R., Matteo, T. D., Khandai, N., & Feng, Y. 2013, MNRAS, 430, 2885
Winters, J. M., Fleischer, A. J., Le Bertre, T., & Sedlmayr, E. 1997, A&A, 326, 305
Wolfire, M. G., McKee, C. F., Hollenbach, D., & Tielens, A. G. G. M. 2003, ApJ, 587, 278
Yamasawa, D., Habe, A., Kozasa, T., Nozawa, T., Hirashita, H., Umeda, H., & Nomoto, K. 2011, ApJ, 735, 44
Yan, H., Lazarian, A., & Draine, B. T. 2004, ApJ, 616, 895
Yasuda, Y., & Kozasa, T. 2012, ApJ, 745, 159
Zhukovska, S., Gail, H. P., Trieloff, M. 2008, A&A, 479, 453

This paper has been typeset from a TEX/ LATEX file prepared by the author.